Title:

In Vitro Uptake and Metabolism of [^{14}C]Acetate in Rabbit Atherosclerotic Arteries: Biological Basis for Atherosclerosis Imaging with [^{11}C]Acetate

Abbreviated title

Metabolism of Acetate in Atherosclerosis (40/45)

Authors:

Kazuaki Yamasaki[1,2], Atsushi Yamashita[3], Yan Zhao[4], Yoichi Shimizu[5,6], Ryuichi Nishii[7,8], Keiichi Kawai[9], Nagara Tamaki[4], Songji Zhao[1], Yujiro Asada[3], Yuji Kuge[5,6]

Affiliations:

[1] Department of Tracer Kinetics & Bioanalysis, Graduate School of Medicine, Hokkaido University, Sapporo, Japan

[2] Department of Nutrition Management, Faculty of Health Science, Hyogo University, Kakogawa, Japan

[3] Department of Pathology, University of Miyazaki, Miyazaki, Japan

[4] Department of Nuclear Medicine, Graduate School of Medicine, Hokkaido University, Sapporo, Japan

[5] Department of Integrated Molecular Imaging, Graduate School of Medicine, Hokkaido University, Sapporo, Japan

[6] Central Institute of Isotope Science, Hokkaido University, Sapporo, Japan

[7] Department of Radiology, Faculty of Medicine, University of Miyazaki, Miyazaki, Japan

[8] Department of Molecular Imaging and Theranostics, National Institute of Radiological Sciences, Chiba, Japan

[9] Division of Health Sciences, Graduate School of Medical Sciences, Kanazawa University, Ishikawa, Japan

Corresponding Author:

Yuji Kuge, PhD

Central Institute of Isotope Science, Hokkaido University,

Kita 15 Nishi 7, Kita-ku, Sapporo 060-8638, Japan

Telephone: 81-11-706-7864

Fax: 81-11-706-7862

E-mail: kuge@ric.hokudai.ac.jp

Keywords

Atherosclerosis / Cardiovascular diseases / [$^{11/14}$C]Acetate / Nuclear medicine diagnosis / Nuclear imaging

Abstract

Introduction:

Detection of vulnerable plaques is critically important for the selection of appropriate treatment and/or the prevention of atherosclerosis and ensuing cardiovascular diseases. In order to clarify the utility of [^{11}C]acetate for atherosclerosis imaging, we determined the uptake and metabolism of acetate by in vitro studies using rabbit atherosclerotic arteries and [^{14}C]acetate.

Methods:

Rabbits were fed with a conventional (n=5) or a 0.5% cholesterol diet (n=6). One side of the iliac–femoral arteries were injured by a balloon catheter. Radioactivity levels in the iliac–femoral arteries were measured after incubation in DMEM containing [1-^{14}C]acetate for 60 min (% dpm/mg tissue). Radioactive components in the homogenized arteries were partitioned into aqueous, organic, and residue fractions by the Folch method, and analyzed by thin-layer chromatography (TLC).

Results:

The radioactivity level in the injured arteries of rabbits fed with the 0.5% cholesterol diet (atherosclerotic arteries) was significantly higher than that in either the non-injured or injured arteries of rabbits fed with the conventional diet (p<0.05) (% dpm/mg tissue:

conventional diet groups; 0.022±0.005 and 0.024±0.007, cholesterol diet groups; 0.029±0.007 and 0.034±0.005 for non-injured and injured arteries). In metabolite analysis, most of the radioactivity was found in the aqueous fraction in each group (87.4–94.6% of total radioactivity in the arteries), and glutamate was a dominant component (67.4–69.7% of the aqueous fraction in the arteries).

Conclusions:

The level of [^{14}C]acetate-derived radioactivity into the arteries was increased by balloon injury and the burden of a cholesterol diet. Water-soluble metabolites were the dominant components with radioactivity in the atherosclerotic lesions. These results provide a biological basis for imaging atherosclerotic lesions by PET using [^{11}C]acetate.

Introduction

Atherosclerosis is the most common cause of cardiovascular diseases. Therefore, it is of critical importance to detect vulnerable plaques for the selection of appropriate treatment and/or the prevention of these diseases [1–3]. Morphological data such as those obtained by computed tomography techniques and/or magnetic resonance imaging have been used for the diagnosis of atherosclerosis [4]. In addition to these morphological data, nuclear medicine can provide functional information of affected tissues, which seems to be useful for the diagnostic evaluation of atherosclerosis and therapy selection.

In this regard, ^{18}F-fluorodeoxyglucose ([^{18}F]FDG), a glucose analog, is widely studied for the evaluation of atherosclerosis [5]. High accumulation of [^{18}F]FDG is observed in vulnerable plaques owing to the increased inflammation in the lesions [6,7]. However, [^{18}F]FDG uptake is largely affected by blood glucose level, which hampers the quantitative assessment of inflammatory states in atherosclerotic plaques in patients with high blood glucose levels including diabetes. Therefore, the development of new diagnostic agents showing accumulation mechanisms different from that of [^{18}F]FDG is strongly required.

Our previous study using metabolomics analysis revealed that the levels of

metabolites such as citrate, fumarate, and malate in the TCA cycle were significantly higher in the injured arteries of rabbits fed with a cholesterol diet than in either the non-injured or injured arteries of rabbits fed with a conventional diet [8]. These results indicate that radiolabeled substrates of the TCA cycle may be utilized for atherosclerosis imaging. From the viewpoint of nuclear medicine, [^{11}C]acetate may be a potential candidate for this purpose, because acetate is metabolized to acetyl-coenzyme A (CoA) and enters the TCA cycle. Indeed, [^{11}C]acetate has been used for the evaluation of TCA cycle activity in the myocardium [9]. Recently, Derlin et al. have shown the potential utility of [^{11}C]acetate for atherosclerosis imaging by clinical research [10]. However, the accumulation mechanisms of [^{11}C]acetate including its metabolites in atherosclerotic lesions remain to be investigated in detail. Although a few previous studies indicated that the incorporation of [^{14}C]acetate into lipid-soluble metabolites such as triglyceride and cholesterol ester was increased in rabbit atherosclerotic lesions owing to enhanced lipid synthesis [11,12], there have been no studies of the contribution of TCA cycle metabolites to the accumulation of radiolabeled acetate in atherosclerotic lesions.

Accordingly, in order to provide a biological basis for atherosclerosis imaging with [^{11}C]acetate and clarify its utility, we determined the uptake and metabolism of acetate by in vitro studies using rabbit atherosclerotic arteries and [^{14}C]acetate.

Materials and Methods

Radiopharmaceutical agents and standards

[1-^{14}C]Acetic acid (37 MBq/ml) was purchased from Perkin Elmer (Boston, MA) and dissolved in Dulbecco's modified Eagle's medium (DMEM). Authentic standards, acetyl coenzyme A, L-glutamic acid, and L-aspartic acid were purchased from Wako Pure Chemical Inc. (Osaka Japan).

Animals

Animal care and all experimental procedures were performed with the approval of the Animal Care Committees of Hokkaido University and Miyazaki University. Eleven male Japanese white rabbits were fed with a conventional (n=5) or a 0.5% cholesterol diet (n=6) and then arterial lesions were induced in the one side of iliac–femoral arteries using a balloon catheter. Three weeks later, the rabbits were subjected to [1-^{14}C]acetate uptake assay [8].

Immunohistochemical analysis

The iliac–femoral arteries were fixed in 4% paraformaldehyde for 12 h at 4 °C and embedded in paraffin. Sections (3 μm thick) were stained with hematoxylin and eosin

and immunohistochemically assessed using antibodies against rabbit macrophages (RAM11; DAKO, Glostrup, Denmark) and smooth muscle actin (1A4; DAKO), a marker of smooth muscle cells (SMCs).

[1-^{14}C]Acetate uptake assay

Rabbits fasted for 4 h were sacrificed by exsanguination under deep pentobarbital anesthesia (60 mg/kg) after the intravenous administration of heparin (500 U/kg). Then, the rabbits were perfused with 50 ml of 0.01 mol/l PBS, followed by 50 ml of DMEM, and their iliac–femoral arteries were rapidly removed and weighed. The arteries were preincubated in DMEM containing 10% fetal bovine serum (FBS) and 37 kBq of [1-^{14}C]acetate was added. After 60 min of incubation, DMEM was removed and the arteries were rinsed three times with PBS, and homogenized on ice. Radioactivity in the homogenized arteries was counted using a liquid scintillation counter (LSC-6100; ALOKA Co., Tokyo, Japan).

Metabolite analysis in arteries

Metabolite analysis was performed using the non-injured or injured iliac–femoral arteries as described in our previous study [13]. The radioactive components in the

homogenized arteries were partitioned into the aqueous, organic, and residue fractions by the Folch method [14], and then radioactivity was measured. The radioactive components in the aqueous layer were then analyzed by thin-layer chromatography (TLC) (silica gel 60; Merck, Darmstadt, Germany) using a solvent system consisting of ethanol: 28% aqueous ammonia (3:1). The TLC plates were exposed to imaging plates, and the exposed plates were analyzed using an image analyzer (FLA-7000; Fuji Photo Film Co., Tokyo, Japan). Radioactive [1-^{14}C]acetate (unchanged compound), acetyl-CoA, glutamate, and aspartate on the TLC plates were identified by comparing with corresponding standards.

Data analysis

All statistical analyses were performed using Stat View version 5.0 (SAS Institute, Inc.). All values are expressed as mean ± standard deviation (SD). In the evaluation of [1-^{14}C]acetate uptake (Fig. 2a and Supplemental Table 1) and metabolite analysis (Fig. 3 and Supplemental Table 2), the Mann–Whitney U test was used. $P<0.05$ was considered to indicate a statistically significant difference.

Results

Histological findings

Figure 1 shows representative histological images obtained three weeks after the balloon injury of the iliac–femoral arteries of rabbits fed with the conventional or 0.5% cholesterol diet. The injured arteries of rabbits fed with the conventional diet showed neointimal formation composed of SMCs. On the other hand, the injured arteries of rabbits fed with the 0.5% cholesterol diet showed the development of an expansive lesion composed of prominently accumulated macrophages and proliferated SMCs. On the other hand, no vascular lesion was induced in the non-injured arteries of the cholesterol- or conventional diet-fed rabbits. It is known that the plaque prone to rupture, a vulnerable plaque, is characterized by macrophage- and lipid-rich core and thin fibrous cap. In contrast, a stable plaque has rich SMCs. Thus, in this study, we defined the injured iliac–femoral arteries of rabbits fed with the 0.5% cholesterol diet as atherosclerotic arteries that mimic vulnerable plaques.

[1-^{14}C]Acetate uptake assay

Figure 2a and Supplemental Table 1 show the radioactivity levels in the iliac–femoral arteries. The radioactivity level in the atherosclerotic arteries was significantly higher

than that in either the non-injured or injured arteries of rabbits fed with the conventional diet. The radioactivity levels in both non-injured and injured arteries were relatively higher in the 0.5% cholesterol diet group than in the conventional diet group. Although the radioactivity level in the conventional diet group was hardly affected by balloon injury, that in the 0.5% cholesterol diet group was slightly increased.

Metabolite analysis in the arteries

The radioactive components in the iliac–femoral arteries were partitioned into the aqueous, organic, and residue fractions by the Folch method (Fig. 2b and Supplemental Table 1). Most of the radioactivity was partitioned into the aqueous fraction (92.6 and 91.7% for non-injured and injured arteries of the conventional diet group, and 94.6 and 87.4% for non-injured and injured arteries of the 0.5% cholesterol diet group, respectively). The radioactivity in the aqueous fraction of rabbits fed with the 0.5% cholesterol diet was significantly higher than that in either the non-injured or injured arteries of rabbits fed with the conventional diet. On the other hand, the percentage of radioactivity in the organic fraction to total radioactivity was negligible. The radioactivity in the organic fraction was significantly higher in the atherosclerotic arteries than in other groups of arteries (Fig. 2b and Supplemental Table 1).

Radioactive acetyl-CoA, aspartate, glutamate, and unchanged compound were determined in the aqueous fraction (Fig. 3 and Supplemental Table 2). Glutamate fraction was a dominant radioactive component of the aqueous fraction (67.4–69.7% of the aqueous fraction). The glutamate fraction was significantly higher in the atherosclerotic arteries than in the non-injured arteries of rabbits fed with the conventional diet. No marked difference was observed in the percentage of radioactivity in each fraction to total radioactivity in the aqueous fraction among the four groups of arteries, including the glutamate fraction (Fig. 3 and Supplemental Table 2).

Discussion

[$^{11/14}$C]Acetate is rapidly transported into cells through the monocarboxylic acid transporters (MCTs) and then metabolized to [$^{11/14}$C]acetyl-CoA by acetyl-CoA synthetase. The generated [$^{11/14}$C]acetyl-CoA condenses with oxaloacetate to form citrate, which then enters the TCA cycle as well as form substrates for lipid synthesis [15,16]. Glutamate and aspartate are synthesized from α-ketoglutarate and from oxaloacetate, respectively, in the TCA cycle (Fig. 4). We considered that our results are relevant to this pathway. Furthermore, our previous metabolomics analysis showed that the level of glutamate as a polarized metabolite was highest in the arteries, and it further increases in the atherosclerotic arteries (data not shown). Thus, the present results of our study using [^{14}C]acetate are consistent with our previous metabolomics analysis. On the other hand, balloon injury and/or the burden of the cholesterol diet did not affect the ratio of radioactivity of each fraction in the water-soluble metabolite (Supplemental Table 2), indicating that enzymes in the TCA cycle are not largely involved in the increased accumulation of [^{14}C]acetate-derived radioactivity in the atherosclerotic arteries.

MCTs, an acetate transporter, are widely distributed in many cells including macrophages and SMCs [17,18]. Particularly, expression level of MCTs in macrophages

is enhanced by various factors such as lipopolysaccharide (LPS) stimulation [18,19]. Thus, the accumulation of acetate-derived radioactivity may reflect the expression levels of MCTs and/or metabolic status of the arteries including subsequent TCA cycle related enzyme.

As for the metabolic aspects of [^{14}C]acetate in atherosclerosis, Charles and Howard showed that the in vitro [^{14}C]acetate-derived radioactivity was higher in the atherosclerotic rabbit aorta than in the control aorta, owing to the enhanced metabolic conversion to cholesterol ester and triglyceride [11]. The enhanced [^{14}C]acetate-derived radioactivity and metabolic conversion to lipid-soluble metabolites in the atherosclerotic arteries were also observed in our present study, indicating an agreement with the results reported by Charles and Howard. On the other hand, our results clearly showed that the contribution of the lipid-soluble metabolites to total radioactivity was small, and water-soluble metabolites largely contribute to [^{14}C]acetate-derived radioactivity in the atherosclerotic lesions. Unfortunately, previous studies [11, 12] did not evaluate the conversion of [^{14}C]acetate to water-soluble metabolites, including TCA cycle intermediates and glutamate. Thus, our results are the first to demonstrate that the increased levels of the water-soluble metabolites are an important factor contributing to the increased uptake level of acetate in atherosclerotic lesions. It should be noted,

however, that the relative change was the largest in the organic fractions (Fig. 2b and Supplemental Table 1). The results clearly indicate the importance of changes in the lipid metabolism in atherosclerotic lesion progression.

Derlin et al. observed the high accumulation level of [^{11}C]acetate-derived radioactivity in the site of predilection for atherosclerosis in human clinical trials. They suggested that enhanced fatty acid synthase function induced by atherosclerosis was a major factor involved in the increased accumulation level [10]. Our results indicate that expression/activity levels of MCTs and subsequent TCA cycle related enzymes, in addition to the enhanced fatty acid synthase function, should be considered to interpret images with [^{11}C]acetic acid in atherosclerotic lesions. The present evidences would provide important biological basis to clarify the potentials of atherosclerosis imaging with [^{11}C]acetic acid and understanding of acetate metabolism, although further clinical and basic studies, including those concerning the roles of MCTs and TCA cycle related enzymes on atherosclerotic lesion progression, are strongly required. In vivo imaging studies in human and experimental animals are also needed to clarify the potentials of atherosclerosis imaging with [^{11}C]acetic acid.

The radioactivity level was relatively higher in the non-injured arteries of rabbits fed with the 0.5% cholesterol diet than in either the non-injured or injured

arteries of rabbits fed with the conventional diet (Fig. 2a). The non-injured and injured arteries were obtained from the same rabbit in our experiment. It seems that the radioactivity level is increased by hyperlipidemia and/or mild intimal injury induced by the burden of the cholesterol diet, even in the non-injured arteries of rabbits fed with the 0.5% cholesterol diet. Thus, our data showed that the increased uptake level of [^{11}C]acetate-derived radioactivity may be seen not only in the advanced and/or vulnerable lesions but also in the early lesions as in the case of [^{18}F]FDG [20], which should be taken into account in the diagnosis of atherosclerosis.

In this study, the coefficient of variation were relatively large. Individual differences in lesion formation may cause the variations. Inhomogeneous lesion formation was observed even in the individual artery, which also seems to cause the variations. In order to solve this problem and to further understand the cells involved in the increase in [^{14}C]acetate accumulation and metabolism, autoradiographic studies with [$^{11/14}$C]acetate and/or immunohistochemical analysis are required. It is also necessary to carry out in vivo imaging using [^{11}C]acetate to confirm the results observed in our in vitro study and the lesion to blood radioactivity ratio. Thereby, we should clarify the clinical importance of incorporation of acetic acid into water-soluble metabolites in the atherosclerotic arteries.

Until now, a number of reports have not mentioned the water-soluble metabolites of [$^{11/14}$C]acetate in atherosclerotic lesions. Our results would provide useful information on the metabolic aspects of [^{11}C]acetate in atherosclerotic lesions.

Conclusions

The level of [^{14}C]acetate-derived radioactivity into the artery was increased by balloon injury and the burden of a cholesterol diet. The water-soluble metabolites of [^{14}C]acetate were the dominant radioactive components in the atherosclerotic lesions. These results provide the biological basis for imaging atherosclerotic lesions by PET using [^{11}C]acetate.

Acknowledgements

This study was performed through the Creation of Innovation Centers for Advanced Interdisciplinary Research Areas Program, Ministry of Education, Culture, Sports, Science and Technology, Japan, and also supported by JSPS KAKENHI (Grant Numbers 26293268, 15K15440, and 16H05163) and the Intramural Research Fund （25-4-3）for Cardiovascular Diseases of the National Cerebral and Cardiovascular Center.

Conflict of Interest Statement

The authors declare that they have no conflict of interest.

Ethical approval

All applicable institutional and/or national guidelines for the care and use of animals were followed.

References

1. Kathryn JM, Ira T. Macrophages in the pathogenesis of atherosclerosis. Cell 2011;145: 341–355.
2. Libby P. Inflammation in atherosclerosis. Nature 2002; 420: 868–874.
3. Koga J, Matoba T, Egashira K. Anti-inflammatory nanoparticle for prevention of atherosclerotic vascular diseases. J Atheroscler Thromb 2016; 23: 757–765.
4. Andor WJM, Riemer HJA, Alessandro B, Elena B, Marcello A, Rudi AJO, et al. Molecular imaging in atherosclerosis. Eur J Nucl Med Mol Imaging 2010; 37: 2381–2397.
5. Zhao Y, Zhao S, Kuge Y, Strauss WH, Blankenberg FG, Tamaki N. Localization of Deoxyglucose and Annexin A5 in Experimental Atheroma Correlates with Macrophage Infiltration but not Lipid Deposition in the Lesion. Mol Imaging Biol 2011; 13: 712–720.
6. Ogawa M, Ishino S, Mukai T, Asano D, Teramoto N, Watabe H, et al. ^{18}F-FDG accumulation in atherosclerotic plaques: immunohistochemical and PET imaging study. J Nucl Med 2004; 45: 1245–1250.
7. Rudd JH, Warburton EA, Fryer TD, Jones HA, Clark JC, Antoun N, et al. Imaging atherosclerotic plaque inflammation with [^{18}F]-fluorodeoxyglucose positron

emission tomography. Circulation 2002; 105: 2708–2711.

8. Yamashita A, Zhao Y, Matsuura Y, Yamasaki K, Moriguchi-Goto S, Sugita C, et al. Increased metabolite levels of glycolysis and pentose phosphate pathway in rabbit atherosclerotic arteries and hypoxic macrophage. PloS One 2014; 9: e86426.
9. Grassi I, Nanni C, Allegri V, James JM, Carlo GM, Castellucci P, et al. The clinical use of PET with ^{11}C-acetate. Am J Nucl Med Mol Imaging 2012; 2: 33–47.
10. Derlin T, Habermann CR, Lengyel Z, Busch JD, Wisotzki C, Mester J, et al. Feasibility of ^{11}C-acetate PET/CT for imaging of fatty acid synthesis in the atherosclerotic vessel wall. J Nucl Med 2011; 52: 1848–1854.
11. Charles F, Howard JR. Lipogenesis from glucose-2-^{14}C and acetate-1-^{14}C in aorta. J. Lipid. Res 1971; 12: 725–730.
12. Day AJ, Wilkinson GK. Incorporation of ^{14}C-Labeled Acetate into Lipid by Isolated Foam Cells and by Atherosclerotic Arterial Intima. Circulation Research 1967; 21: 593–600.
13. Yamasaki K, Zhao S, Nishimura M, Zhao Y, Yu W, Shimizu Y, et al. Radiolabeled BMIPP for Imaging Hepatic Fatty Acid Metabolism: Evaluation of Hepatic Distribution and Metabolism in Mice at Various Metabolic Statuses Induced by Fasting in Comparison with Palmitic Acid. Molecular Imaging 2015; 14.

14. Folch J, Ascoli I, Lees M, Meath JA, Lebaron N. Preparation of lipid extracts from brain tissue. J Biol Chem 1951; 191: 833–841.

15. Klein LJ, Visser FC, Knaapen P, Peters JH, Teule GJ, Visser CA, et al. Carbon-11 acetate as a tracer of myocardial oxygen consumption. Eur J Nucl Med 2001; 28: 651–668.

16. Soloviev D, Fini A, Chierichetti F, Al-Nahhas A, Rubello D. PET imaging with 11C-acetate in prostate cancer: a biochemical, radiochemical and clinical perspective. Eur J Nucl Med Mol Imaging 2008; 35: 942–949.

17. Oikawa K, Iizuka K, Murakami T, Nagai T, Okita K, Yonezawa K, et al. Pure pressure stress increased monocarboxylate transporter in human aortic smooth muscle cell membrane. Mol Cell Biochem 2004; 259: 151-156.

18. Hahn EL, Halestrap AP, Gamelli RL. Expression of the lactate transporter MCT1 in macrophages. Shock 2000; 13: 253-260.

19. Tan Z, Xie N, Banerjee S, Cui H, Fu M, Thannickal VJ, et al. The monocarboxylate transporter 4 is required for glycolytic reprogramming and inflammatory response in macrophages. J Biol Chem 2015; 290: 46-55.

20. Zhao Y, Kuge Y, Zhao S, Strauss HW, Blankenberg FG, Tamaki N. Prolonged high-fat feeding enhances aortic ^{18}F-FDG and ^{99m}Tc-annexin A5 uptake in

apolipoprotein E-deficient and wild-type C57BL/6J mice. J Nucl Med 2008; 49: 1707–1714.

Supplemental Table

Supplemental Table 1. The level of [^{14}C]acetate-derived radioactivity in the arteries and radioactivity partitioned into aqueous, organic, and residue fractions.

Group	Conventional diet		0.5% cholesterol diet	
	Non-injured artery	Injured artery	Non-injured artery	Injured artery
Total Radioactivity (%)	0.022 ± 0.005 (100.0)	0.024 ± 0.007 (100.0)	0.029 ± 0.007 (100.0)	0.034 ± 0.005*† (100.0)
Aqueous fraction (%)	0.021 ± 0.004 (92.6)	0.022 ± 0.006 (91.7)	0.028 ± 0.007 (94.6)	0.030 ± 0.004*† (87.4)
Organic fraction (%)	0.001 ± 0.001 (4.4)	0.001 ± 0.001 (5.3)	0.001 ± 0.001 (3.0)	0.003 ± 0.002*†§ (9.6)
Residue fraction (%)	0.001 ± 0.001 (3.0)	0.001 ± 0.001 (3.0)	0.001 ± 0.001 (2.4)	0.001 ± 0.001 (3.0)

Data represent mean ± SD (% dpm/mg tissue, n=5 for conventional diet group and n=6 for 0.5% cholesterol diet group); * vs non-injured artery (conventional diet); † vs injured artery (conventional diet); § vs non-injured artery (0.5% cholesterol diet). Values in parentheses show the percentage of total radioactivity.

Supplemental Table 2. Metabolite analysis in aqueous fraction.

group	Conventional diet		0.5% cholesterol diet	
	Non-injured artery	Injured artery	Non-injured artery	Injured artery
Aqueous fraction (%)	0.021 ± 0.004 (100.0)	0.022 ± 0.006 (100.0)	0.028 ± 0.007 (100.0)	0.030 ± 0.004*† (100.0)
Acetyl-CoA fraction (%)	0.001 ± 0.001 (5.3)	0.002 ± 0.001 (7.1)	0.001 ± 0.001 (4.4)	0.002 ± 0.001 (6.2)
Aspartate fraction (%)	0.003 ± 0.001 (13.1)	0.002 ± 0.001 (10.4)	0.003 ± 0.001 (12.3)	0.002 ± 0.001 (8.3)
Glutamate fraction (%)	0.014 ± 0.002 (67.4)	0.015 ± 0.004 (68.6)	0.019 ± 0.006 (69.7)	0.020 ± 0.002* (68.3)
Unchanged compound fraction (%)	0.001 ± 0.001 (4.2)	0.001 ± 0.001 (5.6)	0.001 ± 0.001 (3.2)	0.002 ± 0.001 (7.4)
Other compounds fraction (%)	0.002 ± 0.001 (10.0)	0.002 ± 0.001 (8.4)	0.003 ± 0.001 (10.4)	0.003 ± 0.001 (9.9)

Data represent mean ± SD (% dpm/mg tissue, n=5 for conventional diet group and n=6 for 0.5% cholesterol diet group); * vs non-injured artery (conventional diet); † vs injured artery (conventional diet); § vs non-injured artery (0.5% cholesterol diet). Values in parentheses show the percentage of aqueous fraction.

FIGURE LEGENDS

FIGURE 1. Representative immunohistochemical findings of iliac–femoral arteries 3 weeks after balloon injury in rabbits fed with conventional or 0.5% cholesterol diet.

The arterial cross sections were stained with hematoxylin eosin (HE) and antibodies for rabbit macrophage and smooth muscle cells (SMCs). The injured artery in a rabbit fed with the conventional diet shows neointimal formation (N) composed of SMCs. The injured artery in a rabbit fed with the 0.5% cholesterol diet shows the infiltration and accumulation of macrophage (Mϕ) and the proliferation of SMCs with expansive remodeling.

FIGURE 2. Results of (a) [1-^{14}C]acetate uptake assay and (b) the Folch method.

Data represent mean ± SD (DPM/mg tissue, n=5 for conventional diet group and n=6 for 0.5% cholesterol diet group). *p<0.05.

FIGURE 3. Metabolite analysis of aqueous fraction.

Data represent mean (% of radioactivity in each fraction to total radioactivity, n=5 for conventional diet group and n=6 for 0.5% cholesterol diet group). *p<0.05.

FIGURE 4. Potential metabolic pathways of [$^{11/14}$C]acetate for atherosclerosis imaging.

FIGURE 1.

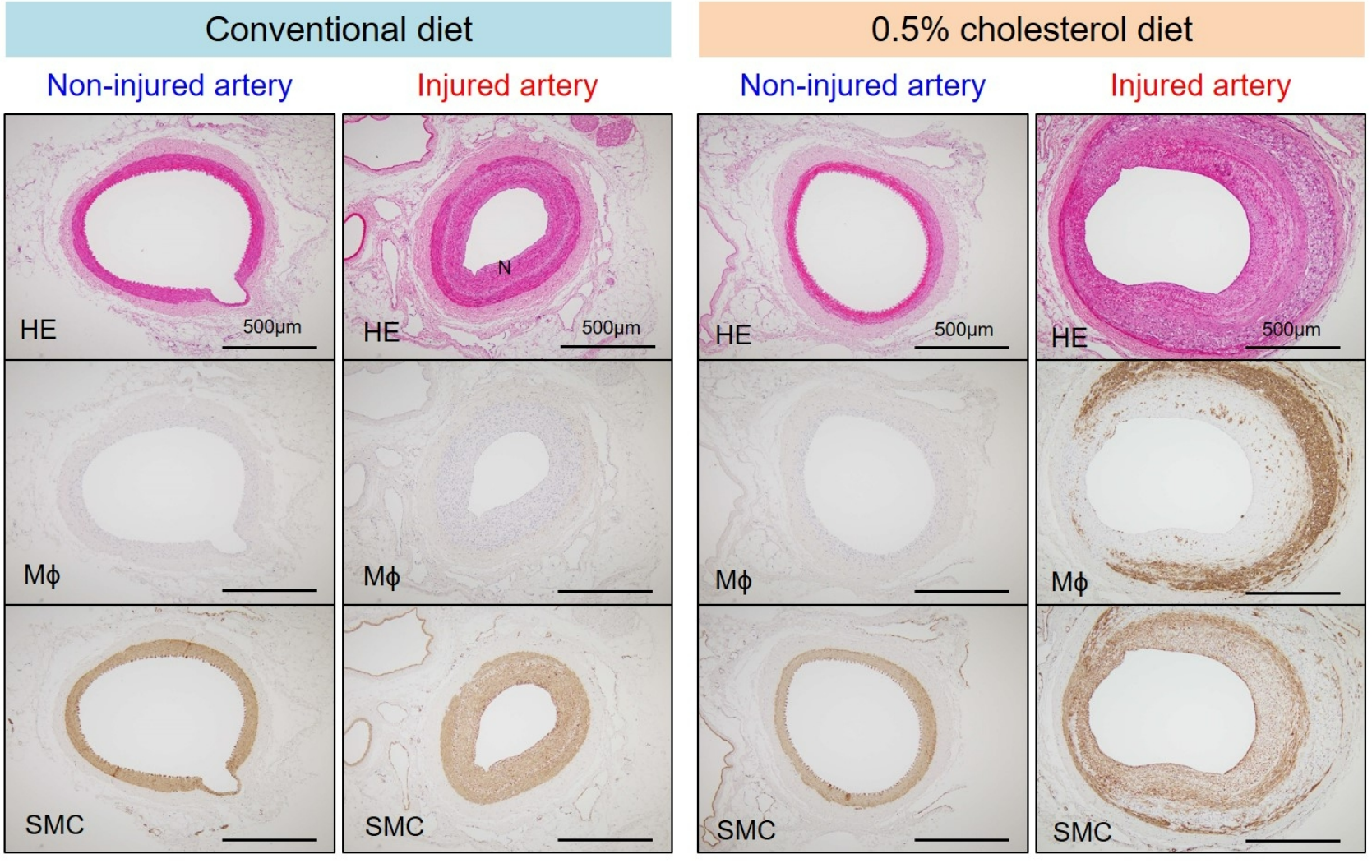
Conventional diet
0.5% cholesterol diet
Non-injured artery
Injured artery
Non-injured artery
Injured artery
HE
500μm
N
HE
500μm
HE
500μm
HE
500μm
Mϕ
Mϕ
Mϕ
Mϕ
SMC
SMC
SMC
SMC

FIGURE 2.

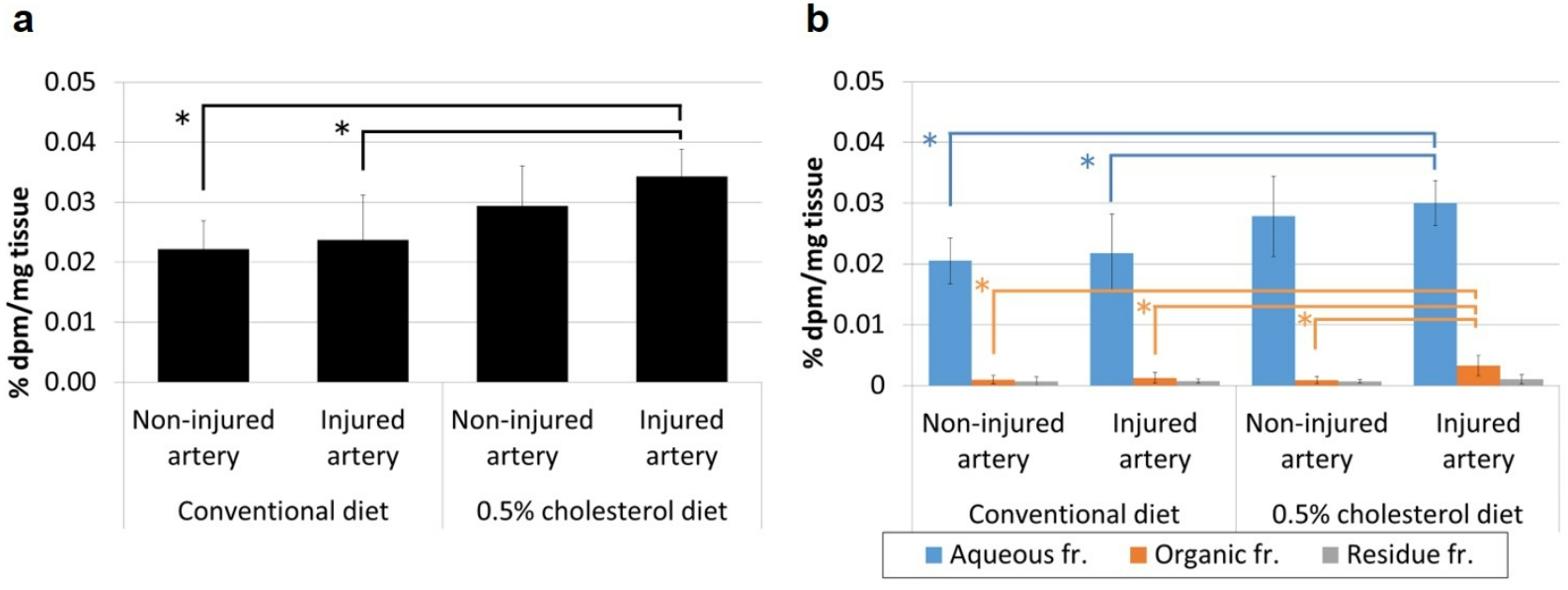
a
0.05
0.04
0.03
0.02
0.01
0.00
% dpm/mg tissue
*
*
Non-injured artery
Injured artery
Non-injured artery
Injured artery
Conventional diet
0.5% cholesterol diet
b
0.05
0.04
0.03
0.02
0.01
0
% dpm/mg tissue
Non-injured artery
Injured artery
Non-injured artery
Injured artery
Conventional diet
0.5% cholesterol diet
Aqueous fr.
Organic fr.
Residue fr.

FIGURE 3.

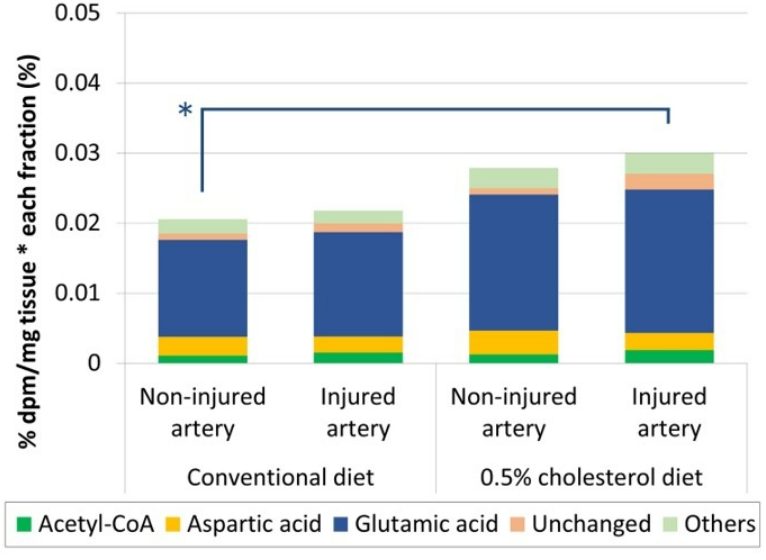
0.05
0.04
0.03
0.02
0.01
0
% dpm/mg tissue * each fraction (%)
*
Non-injured artery
Injured artery
Non-injured artery
Injured artery
Conventional diet
0.5% cholesterol diet
Acetyl-CoA
Aspartic acid
Glutamic acid
Unchanged
Others

FIGURE 4.

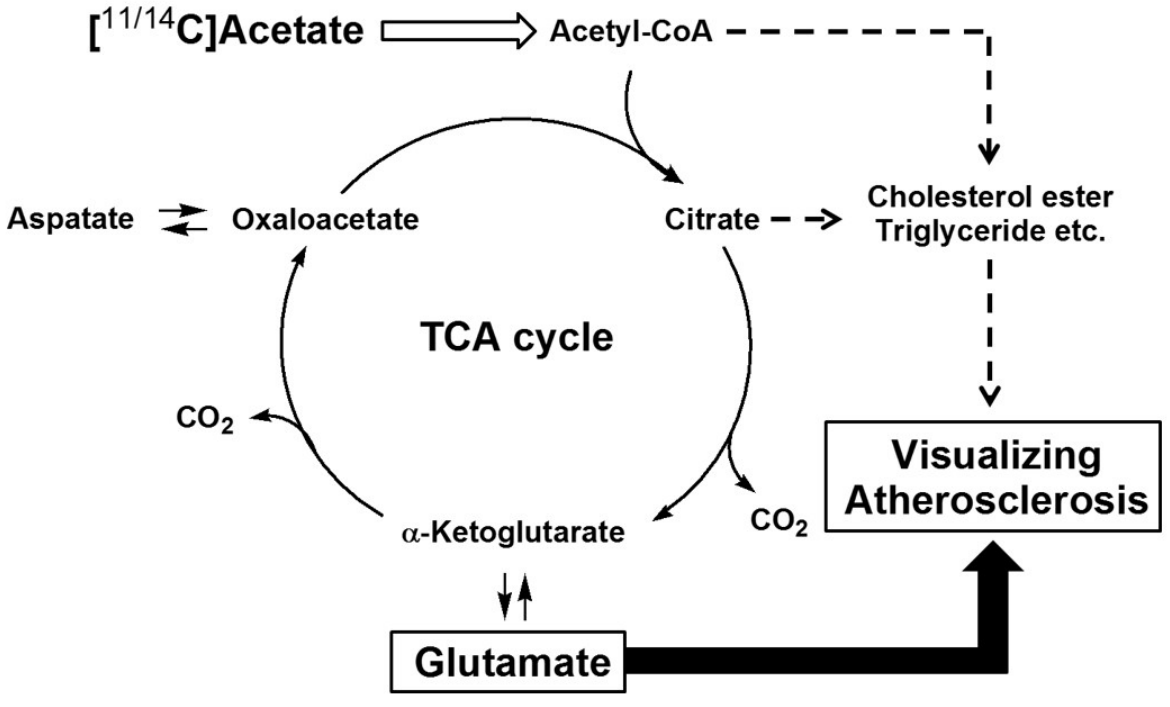
[11/14C]Acetate
Acetyl-CoA
Aspatate
Oxaloacetate
Citrate
Cholesterol ester
Triglyceride etc.
TCA cycle
CO2
CO2
α-Ketoglutarate
Visualizing
Atherosclerosis
Glutamate